Optimal Power Flow for Maximizing Network Benefits From Demand-Side Management

Barry Hayes, *Member, IEEE*, Ignacio Hernando-Gil, *Student Member, IEEE*, Adam Collin, *Member, IEEE*, Gareth Harrison, *Member, IEEE*, and Saša Djokić, *Senior Member, IEEE*

Abstract—This paper applies optimal power flow (OPF) to evaluate and maximize network benefits of demand-side management (DSM). The benefits are quantified in terms of the ability of demand-responsive loads to relieve upstream network constraints and provide ancillary services, such as operating reserve. The study incorporates detailed information on the load structure and composition, and allows the potential network benefits, which could be obtained through management of different load types, to be quantified and compared. It is demonstrated that the actual network location of demand-manageable load has an important influence on the effectiveness of the applied DSM scheme, since the characteristics of the loads and their interconnecting networks vary from one location to another. Consequently, some network locations are more favorable for implementation of DSM, and OPF can be applied to determine the optimal allocation of demand-side resources. The effectiveness of the presented approach is assessed using a time-sequential OPF applied to typical radial and meshed U.K. distribution networks. The results of the analysis suggest that network operators could not just participate in, but also encourage and add value to the implementation of specific DSM schemes at the optimum network locations in order to maximize the total benefit from DSM.

Index Terms—Load management, optimization, power system analysis computing, power system planning, smart grids.

I. INTRODUCTION

FOR several decades, various forms of demand-side management (DSM) have been applied by network operators to regulate system load profiles and to improve system generation-load balancing (e.g., by remote control and block-switching of storage heating loads). These DSM methods were non-locational and affected only the overall system demand, as it was not feasible to control demand within specific areas or locations in the network. In light of the growth in variable renewable power sources and the decreasing contribution of conventional generation to the overall generation portfolio, many studies have identified a need for future networks to provide additional system flexibility through alternative means (e.g., [1]–[4]). DSM has been suggested as having the potential to provide a significant amount of this required flexibility [5], [6]. For instance, it is es-

timated in [1] that as much as 5% of the total Great Britain (GB) system load at winter peak demand could be deferrable, if the necessary DSM technologies and incentives are implemented.

In addition to DSM providing a contribution to system energy balancing, DSM also has significant potential for demand-responsive loads to alleviate network contingencies and manage constraints. An overview of the main concepts and approaches used in "network-driven" DSM (referring to DSM schemes aimed at improving network performance and security) is provided in [7].

The majority of current network-driven DSM initiatives implemented worldwide have been focused on large industrial customers, e.g., [8]–[10], as these users have loads of sufficient size to make a significant contribution to grid ancillary services. In GB, the National Grid requires that users must meet minimum MW and MWh requirements to participate in the Balancing Mechanism (BM), e.g., active power peak demand must be larger than 3 MW at a given site and it has to be reduced by at least 2 hours in order for it to be considered for the provision of certain DSM-based BM services (short-term operating reserve, [8]). However, advances in digital information and communication technologies (ICT), as well as load control at end-use points, are expected to encourage further implementation of DSM amongst smaller customers in other load sectors, e.g., residential and commercial [11]–[13].

In order to achieve the volumes of demand required to participate in the BM and make a significant contribution to network ancillary services, various means of combining and coordinating DSM actions from many highly-distributed users have been proposed, such as the "aggregator" [14] and "virtual power plant" concepts [15], [16]. In addition to the enabling ICT technologies required to realize DSM schemes in the residential and commercial load sectors, new market mechanisms are also required. These electricity market and economic barriers to the further deployment of DSM are discussed in [17] and [18]. The work presented in this paper is focused on the accurate electrical modeling of DSM for the purposes of power system analysis and network support, and not on the electricity market mechanisms, or the enabling ICT infrastructure required for the implementation of the specific DSM actions and schemes discussed.

Since demand side resources in residential and commercial load sectors are highly-distributed and deeply embedded in the LV and MV networks, accurate modeling and analysis of the DSM potential to contribute to the improvement of network performance is a difficult task. The analysis presented in this paper shows that optimal power flow (OPF) can be applied as a planning tool to maximize the network benefits in a given distribution system.

OPF [19] is a well-established technique which is applied for a range of optimization problems in power system operation and planning [20]. As penetrations of variable distributed generation (DG) in networks have increased, OPF formulations have been developed to maximize the amount of variable DG which can be connected to the distribution network without violating voltage, thermal, and fault level constraints [21]–[24]. Furthermore, advanced OPF and linear programming techniques have been proposed for power flow management and asset utilization improvement in distribution networks, e.g., [25]–[28].

OPF techniques have also been applied to minimize the load shedding required in extreme network contingency scenarios, in order to prevent system collapse and/or return the system to secure operation [29]–[36]. However, most of these papers focus on load shedding for improvement of transmission level voltage stability, and the methods developed are not directly applicable to highly-distributed residential and commercial DSM loads.

Recently, there has been considerable interest in the application of OPF methods for optimizing the control of DSM loads and storage devices, where end users are exposed to real-time electricity pricing [37]–[46]. However in many cases, the OPF analysis is not applied to realistic distribution systems, (e.g., [31], [39], [40], [45], [47]), and the impact of the network location of each load on the effectiveness of the DSM schemes is not considered. Additionally, most previous research in the area does not consider in detail the electrical characteristics of typical residential and commercial loads, and the effect of temporal changes in the load structure on the analysis. There have been several papers which discuss the incorporation of more detailed aggregate load models into the OPF [47]–[49]; however, these papers do not deal with DSM applications.

This paper builds on previous work on the modeling and analysis of residential and commercial sector loads described in [50] and [51] to develop a general methodology for assessing the potential network benefits from various DSM-enabled loads in a given distribution network. The presented analysis demonstrates that some network locations are more beneficial for the development and deployment of DSM services than others, due to the electrical characteristics of the loads and their interconnecting networks.

The paper is structured as follows. Section II provides the problem formulation. The proposed methodology is then illustrated in Section III, first using a simple radial distribution network example, and then using a larger, meshed distribution network. Section IV incorporates detailed information on the load structure and load composition in the analysis, while the discussion and conclusions are given in Sections V and VI.

II. PROBLEM FORMULATION

It is demonstrated in [21] that OPF can be used to determine the optimum locations for DG capacity in the distribution network, using the "reverse loadability" technique. This involves adding negative load at each bus iteratively and utilizing the OPF algorithm to maximize the added DG capacity until either the network bus voltage or line constraints are broken. The methodology allows the effects of adding DG at any bus location on the network headroom, or hosting capacity, to be quantified. The analysis in [21] shows that the addition of DG at certain buses is much more beneficial from a network operation point of view, and that connection of DG at inappropriate buses can effectively "sterilize" other parts of the network, i.e., use all of the available headroom and prevent any further DG connections.

A similar, OPF-based approach is applied in this paper, but with a different objective: to determine where the application of demand-manageable loads, or DSM resources, would be of most benefit to the network. The methodology and the results of the analysis suggest that network operators could not just participate in, but also encourage and add value to the implementation of specific DSM schemes at the optimum network locations (e.g., through appropriate economic incentives, or by applying hierarchical/prioritized DSM schemes). The selection of optimal locations for DSM is analogous to the allocation of generator connections and access rights to the network, as implemented by many transmission system operators (TSOs) and distribution network operators (DNOs). Some network operators apply "use of system" charges to encourage generator connections at the most beneficial locations and discourage connections at locations where the network is constrained, or where operational problems may occur. Similar economic incentives could be employed to encourage development of DSM schemes at the optimal network locations. The problem can be stated as follows:

Given a particular network contingency/constraint, and a number of downstream loads, each with a demand-manageable portion, calculate the optimum use of DSM resources which will allow all of the network constraints to be met with the minimum amount of the total load disconnected by a DSM scheme.

A. OPF Constraints and Objective Function

The objective of the OPF formulation is to minimize the total amount of load adjustment required to satisfy network constraints:

$$min \sum_{n=1}^{N_{DSM}} C_n \cdot P_{n,init}(1 - \Psi_n) \qquad (1)$$

where N_{DSM} is the number of network load buses where DSM can be applied, $P_{n,init}$ is the initial active power of bus load n in MW, and Ψ_n represents the load adjustment factor, or the portion of the intitial MW load at bus n which is available for deferral. C_n is the cost of load adjustment assigned to the DSM-enabled load at bus n, in cost units per unit MW. In the analysis presented in this paper, C is not given a monetary value. Instead it is set to an arbitrary value of 1.0 per MW for all of the loads. However, if required, this can be adjusted to allow prices to be set for the various load DSM services that can be offered in a given network (see also Section V).

A full AC-OPF is applied assuming balanced, steady-state conditions, subject to the power flow balance constraints (2)–(3):

$$P_n = \sum_{n=1}^{N} |V_n||V_m|(G_{nm} \cos \theta_{nm} + B_{nm} \sin \theta_{nm}) \quad (2)$$

$$Q_n = \sum_{n=1}^{N} |V_n||V_m|(G_{nm} \sin \theta_{nm} - B_{nm} \cos \theta_{nm}) \quad (3)$$

This article has been accepted for inclusion in a future issue of this journal. Content is final as presented, with the exception of pagination.

HAYES *et al.*: OPTIMAL POWER FLOW FOR MAXIMIZING NETWORK BENEFITS FROM DEMAND-SIDE MANAGEMENT

3

where P_n and Q_n are the real and reactive net power injections at bus n, N is the total number of buses in the system, and G_{nm} and B_{nm} are the real and reactive parts of the elements in the network bus admittance matrix, Y_{bus} corresponding to the nth row and mth column. In addition, the OPF needs to satisfy bus voltage constraints (4), line thermal constraints (5), and constraints on the load adjustment factors at each DSM-enabled bus (6):

$$V_{\min,n} \leq V_n \leq V_{\max,n} \tag{4}$$

$$|S_k| \leq |S_{\max,k}| \tag{5}$$

$$\Psi_{\min,n} \leq \Psi_n \leq \Psi_{\max,n} \tag{6}$$

where $V_{\min,n}$ and $V_{\max,n}$ are the minimum and maximum allowed voltages at each network bus n (including non-load buses), S_k is the MVA power flow through network branch k, and $\Psi_{\min,n}$ and $\Psi_{\max,n}$ are the minimum and maximum load adjustment factors for each load at bus n (based on the proportion of demand-manageable load available).

System load (including the DSM portion) is represented in (1) and (6) by MW demand. The load adjustment factor at each bus, Ψ_n, is expressed as a fraction of the intial bus active power load, $MW_{\text{init},n}$, which is available for deferral. In the examples shown in Section III of this paper, the overall power factor at each load bus is assumed to remain constant as DSM load is disconnected. In practical applications, however, the actual changes in active, reactive and apparent power demand following any DSM action will depend on the type of load which is disconnected. This is considered in Section IV, where a detailed analysis of the changes in load electrical structure due to DSM is provided.

For the OPF analysis, an upstream network contingency is simulated (e.g., thermal overload on an HV line or transformer), and the contribution of each downstream DSM load's ability to bring the constraint under control is compared (all the while maintaining network voltages and power flows within the allowed limits). This analysis could be used to estimate the "value" of DSM load at certain locations in the network, i.e., optimize implementation of DSM at locations where demand-responsive loads have the greatest ability to relieve critical upstream network contingencies.

The OPF formulation outlined in (1)–(6) is a *static* OPF, which is carried out for a single time step, i.e., none of the variables are time-dependent. The presented analysis was implemented in PSS/E [52], which uses an interior point method for OPF calculations.

III. APPLICATION TO NETWORK ANALYSIS

A. Small Radial Distribution Network Example

Fig. 1 shows a typical U.K. radial distribution system, with a small area, serving a mixture of urban and suburban residential and commercial customers, where the feeders are comprised entirely of underground cabling of varying lengths and impedances. The total MW demand for this network at maximum winter loading is 45.5 MW. All data for the modeled 33-, 11-, and 6.6-kV distribution network components are provided by the DNO [53]. The impedances $Z_{eq1} - Z_{eq4}$ represent the equivalent impedances for the typical U.K. urban MV and LV dis-
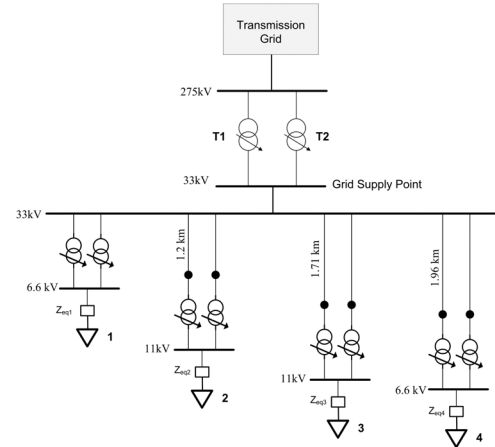

Fig. 1. U.K. radial distribution network model.

TABLE I
LOAD AND NETWORK CHARACTERISTICS
OF A TYPICAL U.K. RADIAL DISTRIBUTION SYSTEM

Bus	Active power demand (MW)	Reactive power demand (MVAr)	Total impedance to GSP, Z (p.u.)
1	7.01	1.88	0.263 + j0.657
2	12.18	3.26	0.468 + j0.815
3	9.32	2.49	0.678 + j0.893
4	16.96	4.54	0.825 + j0.832

tribution networks (the calculation of these equivalent impedances is provided in [54], where more detailed network configurations can also be found). Table I provides the active and reactive power demands at each load bus, and the electrical distances from each load bus to the grid supply point (GSP), $Z_1 - Z_4$, calculated as the total impedance (expressed in per unit on a 100 MVA) from each load to the 33-kV GSP bus.

If one of the 132:33-kV grid supply transformers (e.g., T2 in Fig. 1) is faulted during peak loading conditions, the remaining 132:33-kV transformer (T1) is overloaded, with the MVA flow equal to 105% of the transformer thermal rating. Assuming that there is demand-manageable load at each of the four load buses, the OPF defined in (1)–(6) is applied at each bus in turn to minimize the amount of demand which needs to be adjusted (i.e., disconnected) in order to relieve the overloading of the grid supply transformer, while also maintaining voltages throughout the distribution network within acceptable limits (0.94–1.06 p.u.).

The results of applying the OPF at each load bus are compared in Table II. The amount of load which needs to be disconnected in order to resolve the transformer overload varies at each individual load bus. This is a function of the magnitude of the active and reactive power demands of the loads, and the total impedances of the network connecting each load to the GSP, $Z_1 - Z_4$. Table II shows that the load at Bus 4 only requires 1.26 MW of DSM load to be deferred in order to bring the MVA flow at the grid supply transformer to within its thermal limit (while maintaining all other network constraints within limits), while Bus 1 requires 1.66 MW to be deferred to resolve the same overload. This difference of around 24% is because applying DSM at Bus 4 provides a greater reduction in overall network losses than at Buses 1–3, and therefore implementing DSM at Bus 4

This article has been accepted for inclusion in a future issue of this journal. Content is final as presented, with the exception of pagination.

4   IEEE TRANSACTIONS ON POWER SYSTEMS

TABLE II
RESULTS OF THE OPF AT EACH LOAD BUS

Bus	Load adjustment (MW)
1	-1.66
2	-1.61
3	-1.54
4	-1.26

TABLE III
EFFECTIVENESS INDEX (EI) AND RANKING
OF INDIVIDUAL LOAD BUSES IN EHV4 NETWORK

Bus	Rank	EI	Bus	Rank	EI
1140	1	1.066	1123	9	1.044
1129	2	1.058	1131	10	1.044
1125	3	1.055	...	...	...
6619	4	1.053	306	20	1.019
1139	5	1.051	322	21	1.015
1141	6	1.050	1112	22	1.015
1107	7	1.049	330	23	1.015
6618	8	1.049	316	24	1.000
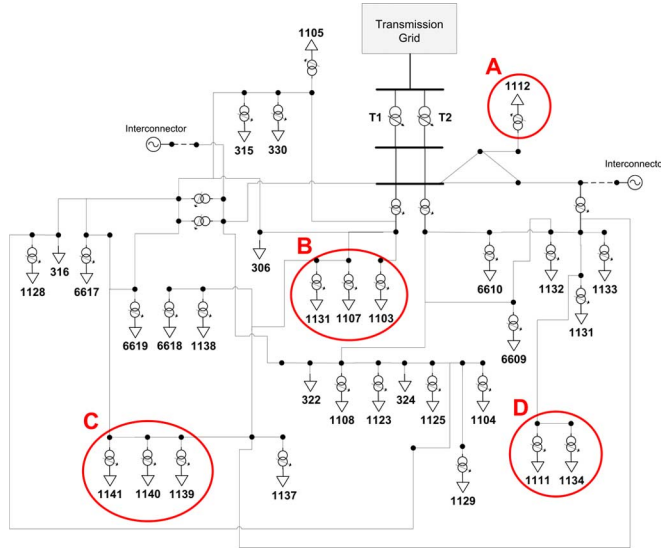
Fig. 2.   UKGDS EHV4 distribution network model [55].

TABLE IV
RESULTS OF THE OPF FOR EACH OF THE LOAD GROUPS A-D

Group	Buses	Total initial load (MW)	Total load adjustment (MW)
A	1112	15.59	-4.51
B	1103, 1107, 1131	20.50	-4.28
C	1139, 1140, 1141	20.13	-4.21
D	1111,1134	11.53	-4.33

provides more benefit to the network than at the other three secondary substations. This result is intuitive and simple to understand, as the example network has a radial configuration.

B. Larger Meshed Distribution Network Example

In a larger, meshed network, with a range of voltage and power flow constraints, the problem of identifying optimal locations for implementing DSM functionalities becomes more complex, but the OPF formulation described above can still be applied to minimize the total load deferral, while meeting all of the network constraints. The following analysis demonstrates the methodology on a well-known test network, the United Kingdom Generic Distribution System (UKGDS) network EHV4 (see [55] for details). This represents a typical U.K. suburban area network, with a mixed construction (combination of overhead lines and cables), and meshed topology. This network comprises 132-, 33-, 11-, and 6.6-kV components with a total combined line length of 85 km, and maximum load of 151.4 MW, Fig. 2.

A similar analysis to that in Section III-A is carried out on the EHV4 network using (1)–(6) to determine which loads are most effective in relieving an upstream network contingency. As in the previous radial network example, the upstream contingency is modeled as a thermal overloading on one of the grid supply transformers. The results are discussed below for DSM schemes implemented at individual load buses and also for the load groups A-D highlighted in Fig. 2.

1) DSM Results for Individual Load Buses: The potential of each individual load bus to provide network benefits (i.e., re-

lief of upstream constraints) can be quantified by an Effectiveness Index (EI), defined as the ratio of load adjustment required at each individual bus compared to the maximum required adjustment across all network buses. For example, at Bus 1140, the load adjustment required to reduce the apparent power flow through the grid supply transformer by 1 MVA (while maintaining all other network constraints within specified limits) is approximately 7% less than the worst-performing bus, Bus 316. The EI ratio is calculated for each load bus in turn and for a range of upstream overloads from 1 to 5 MVA in steps of 0.5 MVA, and the overall average EI is used to rank each load bus in terms of the benefit it provides in reducing MVA flow at the GSP transformer. Table III shows these rankings for the best- and worst-performing load buses in the EHV4 network (buses with a maximum load of less than 2 MW are not considered in the analysis). It is clear from these results that network location also has a significant impact on the effectiveness of DSM schemes for relieving upstream contingencies in the meshed distribution network.

2) DSM Results for Load Groups A-D: In Fig. 2, four load groups located in different parts of the network are highlighted: Group A (Bus 1112), Group B (Buses 1103, 1107 and 1131), Group C (Buses 1139, 1140 and 1141) and Group D (Buses 1111 and 1134). In this case, an overload of 5 MVA at one of the grid supply transformers was simulated, and the OPF is solved to determine the minimum amount of load adjustment required in each of the Groups A-D to resolve the 5-MVA overload at the grid supply point, with results given in Table IV.

It is clear from Table IV that it is more optimal to disconnect DSM load in Group C than in Group A, as only 4.21 MW of user load needs to be disconnected, compared to 4.51 MW in order to relieve the same overload (a difference of around 7%). While the difference between the best- and worst-performing load group is not as large as in the radial network example (Section III-A), the cumulative benefits of implementing a DSM scheme at the

This article has been accepted for inclusion in a future issue of this journal. Content is final as presented, with the exception of pagination.

HAYES *et al.*: OPTIMAL POWER FLOW FOR MAXIMIZING NETWORK BENEFITS FROM DEMAND-SIDE MANAGEMENT

5

TABLE V
LOAD SECTORS IDENTIFIED AT 11-kV SECONDARY SUBSTATIONS
IN TYPICAL U.K. RADIAL DISTRIBUTION NETWORK

Bus	Residential (%)	Commercial (%)	Industrial (%)
1	0	100	0
2	76	14	10
3	28	36	36
4	100	0	0

TABLE VI
COMPARISON OF THE OPF RESULTS AT EACH LOAD BUS

Bus	Load adjustment (MW)			
	Constant Power	Constant Current	Constant Impedance	Actual Load
1	-1.66	-1.68	-1.99	-1.67
2	-1.61	-1.64	-1.98	-1.64
3	-1.54	-1.57	-1.93	-1.59
4	-1.26	-1.35	-1.78	-1.41

loads in Group C rather than Group A over a long period of time are significant.

IV. DETAILED ANALYSIS OF DSM LOAD STRUCTURE AND COMPOSITION

In the previously discussed radial and UKDGS network examples, the aggregate load at each bus is modeled as constant power load type, demanding the same P/Q independent of the voltage conditions. However, the implementation of DSM actions not only reduces the MW magnitude at the selected bus, but also changes the load mix, and hence the electrical characteristics of the aggregate load that remains connected at that bus. The impact of these changes in the load composition on the OPF analysis are discussed in more detail in this section.

A. Comparison of Load Types Applied for DSM

The 11-kV substation loads at each bus in the radial distribution network (Fig. 1) are classified according to the percentage of each of the three main load sectors (residential, commercial and industrial) connected based on measurement data provided by the DNO, Table V. There are also some relatively small contributions from other load sectors, such as street lighting and transportation, but these are neglected since they make up less than 5% of the total aggregate demand.

B. Decomposition of the Aggregate Load

In [50], component-based load models of U.K. residential and commercial sector loads were developed, which allow the aggregate substation demand to be decomposed into its corresponding load components, based on available statistics on load mix and device ownership (e.g., [56]–[58]). The component-based approach described in [50] and [51] is applied in this paper to build an accurate, equivalent representation of the aggregate demand at each bus in the analyzed network, allowing the portion of the demand-manageable load for specific times of the day to be identified. This information allows various DSM scenarios to be modeled by adjusting the corresponding load components in the aggregate demand. Fig. 3 shows the results
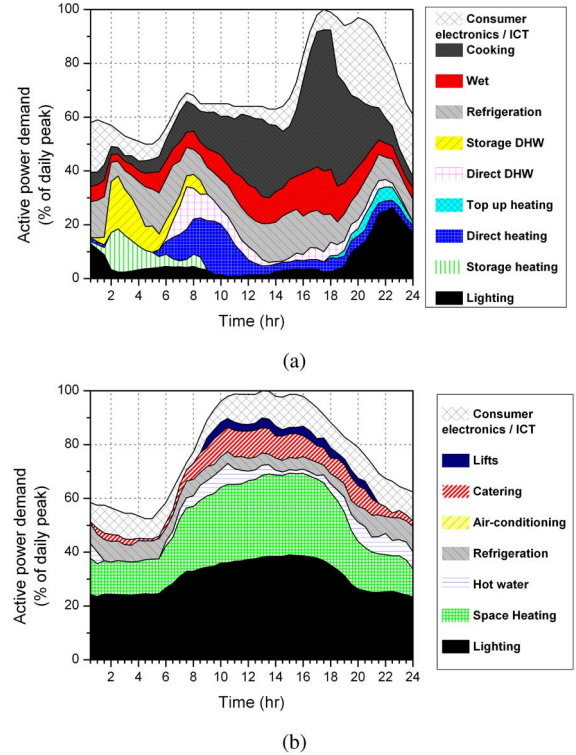

(a)

(b)

Fig. 3. Decomposition of typical UK daily demand curves for maximum winter day: (a) residential sector; (b) commercial sector (ICT stands for information and communications technology, and DHW is domestic hot water).

of the load decomposition for typical U.K. residential and commercial loads, based on demand profiles recorded by the DNO for the maximum winter day. The industrial load model used in this analysis is not decomposed in detail, instead it is assumed constant throughout the day, and is based on the "light industrial" model described in [59].

Using the contributions from each of the three main load sectors, and the decomposition of the aggregate substation demands into load types in Fig. 3, the potential for each load type (e.g., residential "wet" load, commercial refrigeration etc.) to provide network services can be assessed. The aggregated load models are expressed in exponential form, and the analysis is carried out at each 30-min interval, giving a time-varying set of load coefficients, expressing the changes in load composition at each interval over the course of the day:

$$P_t = P_{o,t} \left(\frac{V}{V_o} \right)^{np,t} \quad \text{for } t = 1, \ldots, 48 \tag{7}$$

$$Q_t = Q_{o,t} \left(\frac{V}{V_o} \right)^{nq,t} \quad \text{for } t = 1, \ldots, 48 \tag{8}$$

where np,t and nq,t are the exponential model coefficients at time interval t.

C. Application of Time-Sequential OPF to Analysis of Load Types

A variation of the OPF outlined in (1)–(6) is applied in this section, in order to assess and compare the potential of each *load type* to relieve upstream constraints and congestions. The component-based models of typical residential and commercial U.K. loads described in Section IV-B are used to identify the

This article has been accepted for inclusion in a future issue of this journal. Content is final as presented, with the exception of pagination.

6 IEEE TRANSACTIONS ON POWER SYSTEMS

load types potentially available for DSM, and the times of day at which they are available. The OPF applied is time-sequential, meaning that a static OPF is carried out at each individual time step. However, the OPF formulation does not include inter-temporal constraints, e.g., time dependencies associated with disconnection and reconnection of deferrable loads across multiple time steps. The new objective function is

$$\min C_{l,t} \cdot P_{l,t} \left(1 - \Psi_{l,t}\right) \text{ for } t = 1, \ldots, 48 \quad (9)$$

where $P_{l,t}$ is the active power demand, $\Psi_{l,t}$ is the load adjustment factor and $C_{l,t}$ represents the cost. All variables are defined according to the load type l, at the time interval t. The cost $C_{l,t}$ is set to 1.0 per MW for all loads in the examples shown in this paper, but if required this parameter can be adjusted by the user to provide different values for DSM loads, according to the load type and the time of day at which it is available (see also Section V). The minimization is subject to the same power flow and voltage constraints outlined in (2)–(6), Section II.

The upstream network constraint is again modeled as an overload at the grid supply transformer, and the overloading is increased incrementally until either the amount of DSM load available is exceeded, or one of the network constraints (2)–(5) are broken. The effective MVA reserve at the GSP provided by each load type, defined as S_{reserve}, is expressed as the reduction in MVA flow across the GSP interface. S_{reserve} is calculated simply by subtracting the final MVA flow after the OPF is carried out, $S_{\mathrm{gsp,final}}$, from its initial value, $S_{\mathrm{gsp,init}}$:

$$S_{\mathrm{reserve}} = |S_{\mathrm{gsp,init}}| - |S_{\mathrm{gsp,final}}|. \quad (10)$$

D. Results of Time-Sequential OPF for Each Load Type

The results of the time-sequential OPF are shown Fig. 4, where the effective MVA reserve (10) is calculated for two of the load types identified for DSM: 1) residential "wet" load (this includes domestic washing machines, dishwashers and clothes dryers); 2) commercial refrigeration load. Fig. 4 shows the effective MVA reserve provided by these two load types if applied for DSM at each half-hourly time period, given the assumptions made in Section IV-B for decomposition of the residential and commercial sector load, and taking into account line and transformer losses, as well as voltage and thermal constraints in the distribution network.

The results in Fig. 4 illustrate the amount of MVA reserve which could potentially be obtained from each network bus for the two considered load types, assuming each load type is fully controllable (e.g., 100% of each load type can be disconnected at a given time instant). These results do not consider the reconnection of deferred load, as this will depend on the method by which loads are controlled (e.g., by a price signal, or a frequency control signal to consumer smart appliances). In addition, the actual amount of deferrable load and times for which it is available may vary depending on how the loads are aggregated and coordinated across multiple users in a particular DSM scheme. It is assumed, however, that reconnection of the deferred load will not violate any of the constraints.
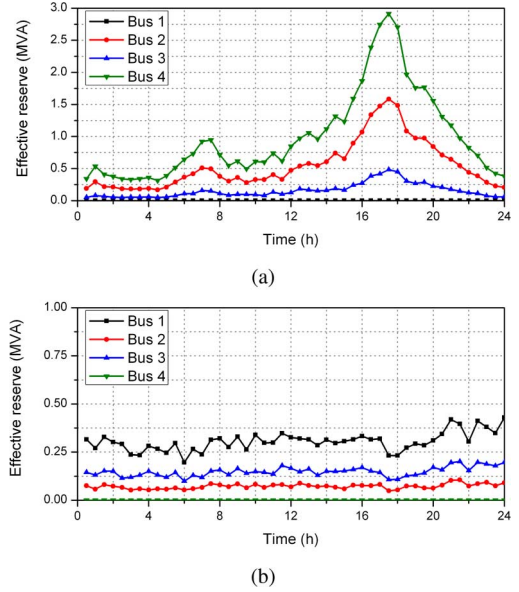

Fig. 4. Effective MVA reserve provided at the GSP by each load type: (a) residential "wet" load; (b) commercial refrigeration load.

E. DSM and Changes in Electrical Characteristics of Aggregate Load

The presented approach allows the effects of any DSM action on the electrical characteristics of the aggregate load to be analysed. The active and reactive exponential coefficients and the aggregate load power factors for Bus 4 are shown in Fig. 5 as instantaneous values at each 30-min interval over the course of day, for both the base case and DSM scenarios (in this case, the DSM scheme disconnects 100% of the available residential "wet" load). As before, the reconnection of the deferred load is not shown.

It is clear from Figs. 5(a) and (b) that there are significant changes in the load exponential coefficients due to the implementation of DSM (particularly in the active power coefficient during afternoon hours). Fig. 5(c) shows that the disconnection of "wet" loads results in a reduction of the aggregate load power factor. Fig. 6 gives the corresponding results at Bus 1, where all commercial refrigeration load is disconnected by the DSM scheme. This figure also shows that the electrical characteristics of the commercial load change as a result of DSM, especially in the early morning ramp period (07:00–09:00). It is important to model changes in the load electrical characteristics due to DSM accurately, since these results may have implications for voltage control and network stability.

F. Comparison of Load Types Applied for DSM

The load mix and its aggregate electrical characteristics can impact the effectiveness of a given DSM scheme. Previously in Section III-A, the amount of load required to be disconnected in order to resolve a transformer overload in the typical U.K. radial urban network was analyzed for each network bus, assuming that all loads are constant power type only (see Table II). The same analysis is repeated in Table VI, this time including
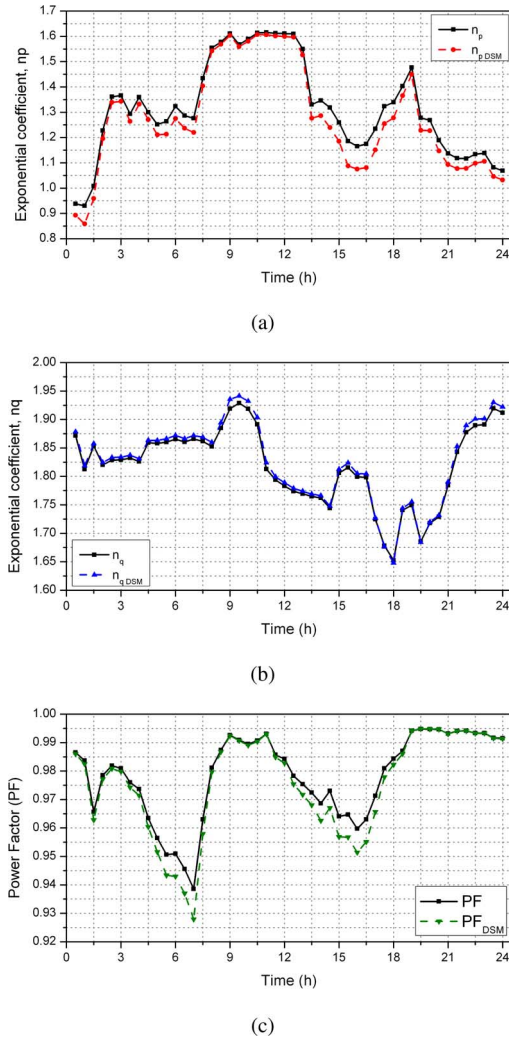
This article has been accepted for inclusion in a future issue of this journal. Content is final as presented, with the exception of pagination.

HAYES *et al.*: OPTIMAL POWER FLOW FOR MAXIMIZING NETWORK BENEFITS FROM DEMAND-SIDE MANAGEMENT   7

Fig. 5. Changes in electrical characteristics of residential load due to disconnection of "wet" load at Bus 4: (a) active power coefficients; (b) reactive power coefficients; (c) power factor.
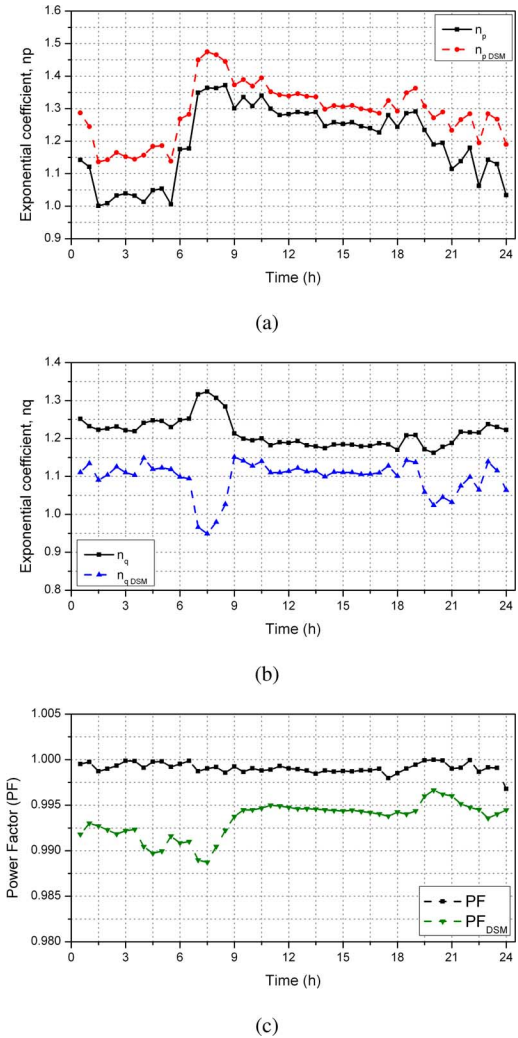

Fig. 6. Changes in electrical characteristics of commercial load due to disconnection of refrigeration load at Bus 1: (a) active power coefficients; (b) reactive power coefficients; (c) power factor.

results for scenarios where all load is modeled as constant current, constant impedance, and finally, using the actual exponential model coefficients calculated at each bus at the daily peak demand, which coincides with the residential peak demand at 17:30–18:00. The results indicate that the detailed composition of load is an important consideration in the OPF analysis, since it impacts the voltages at each load bus and the actual MW/MVAr drawn at each supply point.

V. DISCUSSION

The approach developed in this paper allows the specific contribution of each load type to management of upstream network constraints to be identified. The methodology is extended to include detailed representations of the aggregate load and can be used to analyze the changes in the load electrical characteristics due to DSM actions. It is demonstrated that both the network location and the load composition at each node have a significant impact on the effectiveness of a given DSM scheme. The methodology presented can be applied by network operators as a means for encouraging the development of the most appropriate DSM schemes at the optimal distribution network locations.

Additionally, the cost C in the OPF objective functions (1) and (9), which is set to a default value of 1.0 per MW in this paper, could be adjusted to reflect the actual (or perceived) monetary value of the DSM service provided in a deregulated electricity market. This could allow cost-benefit analysis to be carried out for each load type and allow direct cost per MW/MVA evaluation of ancillary services provided by distributed DSM resources within a given network. In this paper, the time-sequential OPF is applied at each bus or load group individually, in order to compare the effectiveness of implementing DSM at various network locations. The methodology can easily be extended to analyse multiple network nodes simultaneously to find the optimal implementation of DSM at multiple sites across a large network area, and is applicable to both distribution and transmission network studies.

VI. CONCLUSION

This paper applies the OPF technique to evaluate which demand-responsive loads in a given distribution network provide the maximum "value" to the system, in terms of their ability to

relieve upstream network constraints and provide ancillary services, such as operating reserve. The approach is demonstrated on typical U.K. radial and meshed distribution test systems. It is shown that the exact network location of DSM resources has a significant impact on the value that a given deferrable load can provide to the system, in terms of managing upstream constraints. This is due to the different electrical characteristics of the loads, and their interconnecting networks. An OPF-based methodology for evaluating the optimal network locations for DSM is provided, along with an index for ranking each distribution system load bus according to the overall network benefit provided by application of DSM at that bus.

The methodology is extended to incorporate more realistic models of the load composition at each bus, describing the mixture of load types, and the intra-day variations. Detailed, aggregate load models of each of the main load sectors are applied, and a time-sequential OPF is used to determine the effective MVA reserve which could be provided at the GSP interface by each load type. The OPF analysis is carried out using a standard industry tool (PSS/E), and therefore can be readily be applied by network operators to determine which DSM loads, or combination of DSM loads, can provide the maximum benefit to the system in a range of operational scenarios.

The amount of load available for DSM and the length of time for which load could be deferred can vary depending on the exact type of load and how this load is used by the end-users. For instance, the composition of residential and commercial loads may change according to the geographical location, with significant differences between urban, suburban, or rural areas. This makes the identification of "typical" load profiles very difficult. The presented analysis of DSM loads could potentially be improved by adding more load sub-sectors and load types for different end-users, and by more detailed, dynamic modeling of specific load control schemes. The analysis presented in this paper is limited in that it considers each simulation time step separately, and does not include all of the restrictions and time dependencies associated with disconnection and reconnection of various types of deferrable loads. Further work will extend the OPF analysis across multiple time periods in order to model these time dependencies accurately.

REFERENCES

[1] National Grid, "Operating the electricity networks in 2020," National Grid, 2011.
[2] ENTSO-E, Ten Year Network Development Plan, European Network of Transmission System Operators for Electricity, Tech. Rep., 2010.
[3] NERC, Potential Reliability Impacts of Emerging Flexible Resources, North American Electric Reliability Corporation, Tech. Rep., 2010.
[4] IEA DSM, Integration of Demand Side Management, Distributed Generation, Renewable Energy Sources and Energy Storage, International Energy Agency, 2008 [Online]. Available: http://www.ieadsm.org/
[5] C. Geilings, "The concept of demand-side management for electric utilities," Proc. IEEE, vol. 73, pp. 1468–1470, 1985.
[6] A. Keane, A. Tuohy, P. Meibom, E. Denny, D. Flynn, A. Mullane, and M. O'Malley, "Demand side resource operation on the Irish power system with high wind power penetration," Energy Policy, vol. 34, pp. 2925–2934, 2011.
[7] IEA DSM, Assessment and Development of Network Driven Demand Side Management Measures, International Energy Agency, 2008 [Online]. Available: http://www.ieadsm.org/
[8] National Grid, Balancing Services: Demand Side, 2012 [Online]. Available: http://www.nationalgrid.com/uk/Electricity/Balancing/demandside/

[9] D. Loughran and J. Kulick, "Demand side management and energy efficiency in the United States," Energy J., vol. 25, pp. 19–26, 2004.
[10] M. Paulus and F. Borggrefe, "The potential of demand-side management in energy-intensive industries for electricity markets in Germany," Appl. Energy, vol. 88, pp. 432–441, 2011.
[11] G. Strbac, "Demand side management: Benefits and challenges," Elsevier Energy Policy, vol. 36, pp. 4419–4426, 2008.
[12] A. Kiprakis, I. Dent, S. Djokic, and S. McLaughlin, "Multi-scale modeling to maximise demand side management," in Proc. IEEE Innovative Smart Grid Technologies Conf., Manchester, U.K., 2011.
[13] D. Huang and R. Billinton, "Effects of load sector demand side management applications in generating capacity adequacy assessment," IEEE Trans. Power Syst., vol. 27, pp. 335–343, 2012.
[14] J. Medina, N. Muller, and I. Roytelman, "Demand response and distribution grid operations: Opportunities and challenges," IEEE Trans. Smart Grid, vol. 1, pp. 193–198, 2010.
[15] D. Pudjianto, C. Ramsay, and G. Strbac, "Virtual power plant and system integration of distributed energy resources," IET Renew. Power Gen., vol. 1, pp. 10–16, 2007.
[16] N. Ruiz, I. Cobelo, and J. Oyarzabal, "A direct load control model for virtual power plant management," IEEE Trans. Power Syst., vol. 24, pp. 959–966, 2009.
[17] G. Sheble, "Demand is very elastic," IEEE Power and Energy Mag., vol. 9, pp. 14–20, 2011.
[18] M. Albadi and E. El-Saadany, "Demand response in electricity markets: An overview," in Proc. IEEE Power Engineering Society General Meeting, Tampa, FL, USA, 2007.
[19] H. Dommel and W. Tinney, "Optimal power flow solutions," IEEE Trans. Power App. Syst., vol. PAS-87, pp. 1866–1876, 1968.
[20] J. Momoh, R. Adapa, and M. El-Hawary, "A review of selected optimal power flow literature to 1993 (parts 1&2)," IEEE Trans. Power Syst., vol. 14, pp. 96–111, 1999.
[21] G. Harrison and R. Wallace, "Optimal power flow evaluation of distribution network capacity for the connection of distributed generation," IET Gen., Transm., Distrib., vol. 152, pp. 115–122, 2005.
[22] A. Keane and M. O'Malley, "Optimal allocation of embedded generation on distribution networks," IEEE Trans. Power Syst., vol. 20, pp. 1640–1646, 2005.
[23] L. Ochoa, C. Dent, and G. Harrison, "Distribution network capacity assessment: Variable DG and active networks," IEEE Trans. Power Syst., vol. 25, pp. 87–95, 2010.
[24] T. Boehme, G. Harrison, and A. Wallace, "Assessment of distribution network limits for non-firm connection of renewable generation," IET Renew. Power Gen., vol. 4, no. 1, pp. 64–74, 2010.
[25] N. Rau and Y.-H. Wan, "Optimum location of resources in distributed planning," IEEE Trans. Power Syst., vol. 9, pp. 2014–2020, 1994.
[26] A. Keane, L. Ochoa, E. Vittal, C. Dent, and G. Harrison, "Enhanced utilization of voltage control resources with distributed generation," IEEE Trans. Power Syst., vol. 26, pp. 252–260, 2011.
[27] M. Dolan, E. Davidson, I. Kockar, G. Ault, and S. McArthur, "Distribution power flow management utilizing an online optimal power flow technique," IEEE Trans. Power Syst., vol. 27, pp. 790–799, 2012.
[28] S. Gill, I. Kockar, and G. Ault, "Dynamic optimal power flow for active distribution networks," IEEE Trans. Power Syst., vol. 29, pp. 1–11, 2014.
[29] L. Hadju, J. Peschon, W. Tinney, and D. Piercy, "Optimum load-shedding policy for power systems," IEEE Trans. Power App. Syst., vol. PAS-87, pp. 784–795, 1968.
[30] D. Subramanian, "Optimum load-shedding through programming techniques," IEEE Trans. Power App. Syst., vol. PAS-90, pp. 89–95, 1971.
[31] S. Majumdar, D. Chattopadhyay, and J. Parikh, "Interruptible load management using optimal power flow analysis," IEEE Trans. Power Syst., vol. 11, no. 2, pp. 715–720, 1996.
[32] C. Affonso, L. C. P. Da Silva, F. G. M. Lima, and S. Soares, "MW and MVAr management on supply and demand side for meeting voltage stability margin criteria," IEEE Trans. Power Syst., vol. 19, no. 3, pp. 1538–1545, 2004.
[33] M. Rider, C. Castro, V. Paucar, and A. Garcia, "Higher order interior-point method for minimising load-shedding in a competitive electric power market," IET Gen., Transm., Distrib., vol. 151, pp. 433–440, 2004.
[34] E. Aponte and J. Nelson, "Time optimal load shedding for distributed power systems," IEEE Trans. Power Syst., vol. 21, no. 1, pp. 269–277, 2006.
[35] T. Fernandes, J. Lenzi, and M. Mikilita, "Load shedding strategies using optimal load flow with relaxation of restrictions," IEEE Trans. Power Syst., vol. 23, pp. 712–718, 2008.

[36] P. Wang, Y. Ding, and L. Goel, "Reliability assessment of restructured power systems using optimal load shedding technique," *IET Gen., Transm., Distrib.*, vol. 3, pp. 628–640, 2009.

[37] W. Uturbey and A. Costa, "Dynamic optimal power flow approach to account for consumer response in short term hydrothermal coordination studies," *IET Gen., Transm., Distrib.*, vol. 1, pp. 414–421, 2007.

[38] K. Chandy, S. Low, U. Topcu, and H. Xu, "A simple optimal power flow model with energy storage," in *Proc. 49th IEEE Conf. Decision and Control (CDC)*, 2010, pp. 1051–1057.

[39] N. Gudi, L. Wang, V. Devabhaktuni, and S. Depuru, "A demand-side management simulation platform incorporating optimal management of distributed renewable resources," in *Proc. 2011 IEEE/PES Power Systems Conf. Expo. (PSCE)*, 2011, pp. 1–7.

[40] N. Li, L. Chen, and S. Low, "Optimal demand response based on utility maximization in power networks," in *Proc. 2011 IEEE Power and Energy Society General Meeting*, 2011, pp. 1–8.

[41] N. Li, L. Gan, L. Chen, and S. Low, "An optimization-based demand response in radial distribution networks," in *Proc. 2012 IEEE Globecom Workshops (GC Wkshps)*, 2012, pp. 1474–1479.

[42] A. Gabash and P. Li, "Active-reactive optimal power flow in distribution networks with embedded generation and battery storage," *IEEE Trans. Power Syst.*, vol. 27, pp. 2026–2035, 2012.

[43] Z. Chen, L. Wu, and Y. Fu, "Real-time price-based demand response management for residential appliances via stochastic optimization and robust optimization," *IEEE Trans. Smart Grid*, vol. 3, no. 4, pp. 1822–1831, 2012.

[44] P. Siano, C. Cecati, H. Yu, and J. Kolbusz, "Real time operation of smart grids via FCN networks and optimal power flow," *IEEE Trans. Ind. Informat.*, vol. 8, no. 4, pp. 944–952, 2012.

[45] E. Sanseverino, M. Di Silvestre, G. Zizzo, and G. Graditi, "Energy efficient operation in smart grids: Optimal management of shiftable loads and storage systems," in *Proc. 2012 Int. Symp. Power Electronics, Electrical Drives, Automation and Motion (SPEEDAM)*, 2012, pp. 978–982.

[46] C. Cecati, C. Buccella, P. Siano, and A. Piccolo, "Optimal operation of smart grids with demand side management," in *Proc. 2013 IEEE Int. Conf. Industrial Technology (ICIT)*, 2013, pp. 2010–2015.

[47] X. Li, Y. Li, and S. Zhang, "Analysis of probabilistic optimal power flow taking account of the variation of load power," *IEEE Trans. Power Syst.*, vol. 23, no. 3, pp. 992–999, 2008.

[48] L. G. Dias and M. E. El-Hawary, "Effects of load modeling in security constrained OPF studies," *IEEE Trans. Power Syst.*, vol. 6, no. 1, pp. 87–93, 1991.

[49] L. G. Dias and M. El-Hawary, "OPF incorporating load models maximizing net revenue," *IEEE Trans. Power Syst.*, vol. 8, no. 1, pp. 53–59, 1993.

[50] A. Collin, J. Acosta, I. Hernando-Gil, and S. Djokic, "An 11 kV steady state residential aggregate load model (Parts 1&2)," in *Proc. 2011 IEEE PowerTech*, Trondheim, Norway, 2011.

[51] B. Hayes, A. Collin, I. Hernando-Gil, J. Acosta, S. Hawkins, G. Harrison, and S. Djokić, "All-scale modelling of wind generation and responsive demand in power system studies," in *Proc. IEEE PES General Meeting*, San Diego, CA, USA, 2012.

[52] Siemens Energy, Power System Simulator for Engineering, 2012 [Online]. Available: http://www.ptius.com/pti/software/psse/index.cfm

[53] Scottish Power Distribution, SP Distribution Long Term Development Statement, 2011.

[54] I. Hernando-Gil, I. Ilie, and S. Djokic, "Reliability performance of smart grids with demand-side management and distributed generation/storage technologies," in *Proc. IEEE PES Innovative Smart Grid Technologies Conf. (ISGT Europe)*, Berlin, Germany, 2012.

[55] United Kingdom Generic Distribution System, 2006 [Online]. Available: http://monaco.eee.strath.ac.uk/ukgds/

[56] Department of Energy and Climate Change, 2011, Subnational Electricity Consumption Data, Regional and Local Authority Electricity Consumption Statistics: 2005–2010 [Online]. Available: http://www.decc.gov.uk/en/content/cms/statistics/energy stats/

[57] Department of Energy and Climate Change, 2012, Digest of UK Energy Statistics [Online]. Available: http://www.decc.gov.uk/en/content/cms/statistics/publications/dukes/

[58] C. Pout, F. MacKenzie, and E. Olluqui, The Impact of Changing Energy Patterns in Buildings on Peak Electricity Demand in the UK, Department of Energy and Climate Change, Tech. Rep., 2008.

[59] EPRI, Advanced Load Modeling: Entergy Pilot Study, EPRI, Palo Alto, CA, USA and Entergy Inc., New Orleans, LA, USA, Tech. Rep., 2004, 1011391.

Barry Hayes (S'09–M'12) received the B.Eng. degree in electrical and electronic engineering from University College Cork, Ireland, in 2005, the M.Eng. degree from the National University of Ireland Maynooth in 2008, and the Ph.D. degree in power systems from the University of Edinburgh, Edinburgh, U.K., in 2013.

He is currently a Marie Curie Postdoctoral Research Fellow at the IMDEA Energy Institute in Madrid, Spain. He has also worked as a Research Fellow at the University of Edinburgh, and in industry with Intel Ireland and National Grid UK. His main research interests are network integration of renewable energy sources and planning and operation of future power distribution systems.

Ignacio Hernando-Gil (S'10) received the B.Eng. degree in industrial engineering (electrical and electronic specialization) from Polytechnic University of Madrid, Spain, in 2008 and the M.Sc. degree in energy from Heriot-Watt University, Edinburgh, U.K., in 2009. He is currently pursuing the Ph.D. degree at the University of Edinburgh, Edinburgh, U.K.

He has worked as a Research Fellow at the Institute for Energy Systems, University of Edinburgh. His research is focused on power system modeling and analysis, including the assessment of quality of supply in future electricity networks.

Adam Collin (S'10–M'12) received the B.Eng. degree in electrical and electronic engineering from the University of Edinburgh, Edinburgh, U.K., in 2007, the M.Sc. degree in renewable energy and distributed generation from Heriot-Watt University, Edinburgh, U.K., in 2008, and the Ph.D. degree from the University of Edinburgh in 2013.

He is currently employed as a research fellow at the Institute for Energy Systems, University of Edinburgh. His research interests include load modeling and their influence on the analysis of distribution system performance.

Gareth Harrison (M'02) is Bert Whittington Chair of Electrical Power Engineering at the University of Edinburgh, Edinburgh, U.K. His current research interests include network integration of renewable generation and analysis of the impact of climate change on the electricity industry.

Prof. Harrison is a Chartered Engineer and member of the Institution of Engineering and Technology, U.K.

Saša Djokić (M'05–SM'11) received the Dipl.Ing. and M.Sc. degrees in electrical engineering from the University of Nis, Nis, Serbia, and the Ph.D. degree in the same area from the University of Manchester Institute of Science and Technology (UMIST, now the University of Manchester), Manchester, U.K.

From 1993 to 2001, he was with the Faculty of Electronic Engineering of the University of Nis. From 2001 to 2005, he was with the School of Electrical and Electronic Engineering at the UMIST/University of Manchester. Currently, he is a Reader in the School of Engineering, University of Edinburgh, Edinburgh, U.K.